Available online at www.sciencedirect.com

SCIENCE DIRECT

Biochimica et Biophysica Acta 1744 (2005) 224 – 233

BIOCHIMICA ET BIOPHYSICA ACTA

BBA

http://www.elsevier.com/locate/bba

Vasoactive intestinal peptide (VIP) induces c-*fos* expression in LNCaP prostate cancer cells through a mechanism that involves Ca^{2+} signalling. Implications in angiogenesis and neuroendocrine differentiation

Beatriz Collado, María G. Sánchez, Inés Díaz-Laviada, Juan C. Prieto*, María J. Carmena

Department of Biochemistry and Molecular Biology, Alcalá University, Alcalá de Henares 28871, Spain

Received 3 December 2004; received in revised form 30 March 2005; accepted 15 April 2005
Available online 16 May 2005

Abstract

The effect of vasoactive intestinal peptide (VIP) on intracellular Ca^{2+} levels and its relationship with the expression of c-*fos* and vascular endothelial growth factor (VEGF) as well as with neuroendocrine (NE) differentiation were investigated in human prostate LNCaP cells. VIP induced the expression of c-*fos* mRNA as studied by reverse transcription polymerase chain reaction (RT-PCR). It was accompanied by VIP stimulation of c-*fos* protein synthesis, as measured by Western blot analysis. VIP enhanced intracellular Ca^{2+} levels as evaluated using the calcium probe fura-2. VIP regulation of c-*fos* expression depended on $[Ca^{2+}]_i$ concentration since the intracellular calcium chelator BAPTA/AM decreased c-*fos* expression (both mRNA and protein) to basal levels. As shown by means of real-time RT-PCR, VIP stimulated VEGF mRNA expression: the effect was inhibited by 40% in the presence of curcumin (an inhibitor of AP-1 binding), and it was dependent on Ca^{2+} since BAPTA/AM inhibited this VIP action by 43%. Similar observations were made on the effects of BAPTA/AM and curcumin on VIP stimulation of VEGF protein expression. Simultaneous treatment of cells with the protein kinase A inhibitor H89 and BAPTA/AM completely blocked this VIP effect, whereas each agent alone led only to a partial inhibition. In addition, the calcium chelator blocked by 37% the ability of VIP to induce NE cell differentiation as estimated by the observation of neurite development. These features support a VIP signalling pathway that could be mediated through both cAMP and $[Ca^{2+}]_i$ increase in prostate LNCaP cancer cells. Moreover, our data suggest the implication of c-Fos on the induction of the main angiogenic factor VEGF since the promoter region of the VEGF gene possesses AP-1 (i.e., c-Fos/c-Jun heterodimer) response elements. This feature represents a link between the nuclear oncogene c-*fos*, angiogenesis and NE differentiation by means of an initiating signal upon VIP receptors.

Keywords: VIP receptor; Prostate cancer; c-*fos*; Ca^{2+}; cAMP; VEGF

1. Introduction

The vasoactive intestinal peptide (VIP) is a pleiotropic neuropeptide that binds to two classes of membrane receptors ($VPAC_1$ and $VPAC_2$ receptors) that are preferentially coupled to $G\alpha_s$ protein and activates adenylyl cyclase in many tissues [1] including the prostate gland [2,3]. Increased cAMP levels may activate protein kinase A resulting in phosphorylation of protein substrates such as the cAMP response element binding protein (CREB) [4]. CREB phosphorylation leads to increased expression of c-*fos*, c-*jun*, and c-*myc* oncogenes. Whereas cAMP is the main second messenger in VIP activity, the involvement of Ca^{2+} in VIP signalling pathways has been less investigated. Both $VPAC_1$ and $VPAC_2$ receptors are able to couple to the IP_3/Ca^{2+} pathway through Gq and $G\alpha_i$ proteins and thus enhancing $[Ca^{2+}]_i$ levels [5–8].

VIP behaves as a trophic factor in many cancer cell types [9]. We have recently demonstrated that VIP, mostly

* Corresponding author. Tel.: +34 91 8854 527; fax: +34 8854 585.
E-mail address: juancarlos.prieto@uah.es (J.C. Prieto).

0167-4889/$ - see front matter © 2005 Elsevier B.V. All rights reserved.
doi:10.1016/j.bbamcr.2005.04.009

through $VPAC_1$ receptors, increases the expression of the major angiogenic factor, vascular endothelial growth factor (VEGF) [10], and induces neuroendocrine (NE) differentiation [11] in the human androgen-dependent lymph node carcinoma of the prostate LNCaP cell line. Moreover, VIP protects from apoptosis in an androgen-independent prostate cancer cell line (PC-3) [12]. Angiogenesis, NE differentiation, and survival of cells are three steps involved in prostate cancer progression to the hormone-independence stage, which is more aggressive and presents a poor prognostic. Both VIP and VIP receptors are abundant in autonomic nerve fibres of human prostate and in NE-differentiated prostate carcinoma cells [13] which support their potential role as possible therapeutic targets in prostate cancer, the sixth most common cancer in the world and the third leading cause of cancer in men [14,15].

Adenylyl cyclase is the primary signal transduction pathway of VIP receptors in both normal prostate and prostate cancer cells [1,12,16]. However, the effects of VIP on VEGF expression and NE differentiation in prostate LNCaP cells involve different signalling pathways, including both PKA-dependent and -independent mechanism [10]. Furthermore, the short time needed for these VIP effects suggests the involvement of other early signals that would induce angiogenesis and NE phenotype in prostate cancer cells. In this context, VIP induces c-*fos* mRNA expression by a cAMP-independent mechanism in GH_3 cells [17], and the VIP-related peptide pituitary adenylate cyclase-activating peptide (PACAP) activates the heterodimeric transcription factor AP-1 (activator protein 1) in rat pancreatic carcinoma cells [18]. AP-1 contains members of the Jun, Fos, Atf (activating transcription factor), and Maf (musculoaponeurotic fibrosarcoma) protein families, which can form different dimer combinations through their leucine-zipper domains and thus recognize different sequence elements in the promoters and enhancers of target genes. The main AP-1 proteins in mammalian cells are Fos and Jun, but c-Fos by itself does not form a homodimer or bind with DNA since its transactivating activity depends on its association to c-Jun family members to form the corresponding AP-1 complex that binds to the DNA backbone [19]. The formation of this complex, Fos-Jun-DNA, is inhibited by curcumin, the yellow pigment of turmeric, which has anti-angiogenic activity [20]. The c-*fos* oncogene is an earlier response gene which can be activated by several stimuli, including serum, growth factors, hormones, and Ca^{2+}. The early effect of VIP on $VEGF_{165}$ expression in prostate cancer LNCaP cells [10] is consistent with a direct action on the promoter region of VEGF gene that possesses several potential transcription binding sites. Interestingly, the promoter region of VEGF gene possesses five response AP-1 elements [21]. The purpose of the present study was to analyze the mechanisms by which VIP induced expression and NE differentiation in prostate cancer LNCaP cells. We present evidence on that VIP-induced Ca^{2+} signalling is involved in these events as well as in c-*fos* expression stimulation.

2. Materials and methods

2.1. Materials

Synthetic VIP was purchased from Neosystem (Strasbourg, France). Purified goat polyclonal anti-c-Fos antibody and the secondary antibodies were horseradish peroxidase-conjugated, and were obtained from Santa Cruz Biotechnologies (Santa Cruz, CA, USA). Bis-(2-aminophenoxy)ethane-*N*,*N*,*N*′,*N*′-tetraacetic acid acetoxymethyl ester (BAPTA/AM) was purchased from Calbiochem (Schwalbach, Germany), and N-(2-(p-bromocinnamylamino)ethyl)-5-isoquinolinesulfonamide (H89) from Alexis (Grünberg, Germany). Other chemicals were purchased from Sigma (Alcobendas, Spain).

2.2. Cell culture

The androgen-dependent human prostate cancer cell line LNCaP was purchased from the American Type Culture Collection (Rockville, MD, USA). Cells were routinely cultured in RPMI-1640 medium supplemented with 10% heat-inactivated foetal bovine serum (FBS) and 1% penicillin/streptomycin/amphotherycin B (Life Technologies, Barcelona, Spain) at 37 °C in humidified 5% CO_2 environment. For experiments, cells were seeded at a density of 30,000–40,000 cells/cm^2. The culture medium was changed every 3 days.

2.3. Isolation of total RNA and reverse transcription polymerase chain reaction (RT-PCR)

LNCaP cells (2×10^6 cells in 100 mm cell culture dishes) were stimulated with 0.1 μM VIP for 1 h after 1 h of pretreatment in the presence or absence of either 10 μM curcumin or 60 μM BAPTA/AM. Total cell RNA was isolated with Ultraspec RNA reagent (Biotecx Labs, Houston, TX, USA) according to the instructions of the manufacturer. Two μg of total RNA were reverse-transcribed using 6 μg of hexamer random primers and 200 U M-MLV RT (Life Technologies) in the buffer supplied with the enzyme supplemented with 10 nM dithiotreitol, 40 U RNasin (Promega, Madison, WI, USA) and 0.5 mM of deoxyrybonucleotides (dNTPs). Four microliters of RT reaction were then PCR-amplified with specific primers for c-fos: sense 5′-AAG GAG AAT CCG AAG GGA AAG GAA TAA GAT GGC T-3′, and antisense 5′-AGA CGA AGG AAG ACG TGT AAG CAG TGC AGC T-3′. PCR-conditions were: denaturation at 94 °C for 5 min, followed by 28 cycles of 95 °C for 35 s, 58 °C for 40 s, 72 °C for 40 s, and then a final cycle of 10 min at 72 °C. The signals were normalized with the β-actin gene expression level; the

primers for β-actin were: sense 5′-AGA AGG ATT CCT ATG TGG GCG-3′ and antisense 5′-CAT GTC GTC CCA GTT GGT GAC-3′. The PCR products were separated by electrophoresis and visualized in 2% agarose gels. The bands were cut from the gel, eluted, and automatically sequenced with an ABI 377 sequencer (Applied Biosystems, Foster City, CA, USA).

2.4. Single-step real-time RT-PCR

Real-time quantitative RT-PCR analysis was carried out using 50 ng of RNA for each sample and SYBR Green PCR master mix (Applied Biosystems) in one-step RT-PCR protocol according to the manufacturer's instructions. The thermal cycling conditions were 30 min at 48 °C for RT and 10 min at 95 °C to activate AmpliTaq Gold DNA Polymerase, followed by 40 cycles of 95 °C for 15 s and 60 °C for 1 min. Primers were chosen with the assistance of the computer program Primer Express (Perkin-Elmer Applied Biosystems, Foster City, CA, USA). The PCR amplicon region for VEGF contained the splice variant $VEGF_{165}$. Primers for $VEGF_{165}$ were: sense 5′-GAC AAG AAA ATC CCT GTG GGC-3′ and antisense 5′-AAC GCG AGT CTG TGT TTT TGC-3′. The relative quantification was normalized to β-actin. PCR reaction was carried out using ABI-Prism 7000 SDS (Perkin Elmer Applied Biosystems). The presence of the PCR products was verified by electrophoresis separation and visualization in 2% agarose gels. The corresponding bands were cut from the gel, eluted, and automatically sequenced by an ABI 377 sequencer (Applied Biosystems). Results of real-time PCR were represented as *C*t values, where *C*t was defined as the threshold cycle number at which product is first detected by fluorescence. The amount of target ($VEGF_{165}$) was normalized to an endogenous reference, the housekeeping gene for β-actin. Δ*C*t was the difference in *C*t values derived from the $VEGF_{165}$ gene in each sample assayed, and β-actin gene. ΔΔ*C*t represented the difference between the paired samples. The *n*-fold differential ratio was expressed as $2^{-\Delta\Delta Ct}$ [22].

2.5. Protein isolation and Western blotting

LNCaP cells (2×10^6 cells in 100 mm cell culture dishes) were stimulated with 0.1 μM VIP for different time periods. Cells were washed twice with ice-cold PBS and then harvested, scraped into ice-cold PBS, and then pelleted by centrifugation at 500×*g* for 5 min at 4 °C. For preparation of nuclear and cytosolic extracts [23], the packed cells were resuspended into 10 mM Tris–HCl (pH 7.5), 1.5 mM $MgCl_2$, and 10 mM KCl freshly supplemented with 2 mM dithiothreitol (DTT), 0.4 mM phenyl methylsulfonylfluoride (PMSF), 2 μg/ml leupeptin, 2 μg/ml aprotinin, 2 μg/ml pepstatin, and 1 mM Na_3VO_4. Cells were kept on ice for 10 min, and then nuclei were pelleted by centrifugation at 17,000×*g* for 10 min at 4 °C. The cytosolic extract was kept, and the pellet was resuspended into 20 mM Tris–HCl buffer (pH 7.5) containing 0.5 M NaCl, 20% glycerol and 1.5 mM $MgCl_2$, freshly supplemented with the protease and phosphatase inhibitors listed above, and rotated for 30 min in cold room. The extract was cleared by centrifugation at 20,000×*g* for 30 min at 4 °C. Proteins (18–20 μg) from cytosolic or nuclear extracts were resolved by 10% SDS-PAGE, blotted onto a nitrocellulose membrane (BioTrace® NT, Pall Corporation, Ann Arbor, MI, USA), and incubated with the corresponding primary antibody. Immunoreactivity was detected with horseradish peroxidase-conjugated secondary antiserum followed by treatment with enhanced chemiluminescence reagent (Pierce Biotechnology, Rockford, IL, USA). β-actin antibody was used as loading control.

2.6. Determination of VEGF

$VEGF_{165}$ secretion by LNCaP cells to culture medium was quantified by an enzyme-linked immunosorbent assay (ELISA) (R&D Systems, Minneapolis, MN, USA). LNCaP cells were placed in 6-multiwell plates at a density of 350,000 cells/well in complete medium for 24 h. Then, cells were stimulated for 1 h with 60 μM BAPTA/AM or 10 μM curcumin, or for 15 min with H89; thereafter, cells were stimulated for 8 h with 0.1 μM VIP. Finally, the supernatants were taken for VEGF assay according to the instructions of the manufacturer.

2.7. Calcium measurements

Cytosolic calcium concentration variations were measured using the calcium probe fura-2. LNCaP cells were plated overnight at a density of 40,000 cells/ml on glass coverlips. The cells were then washed with RPMI 1640 containing 0.1% bovine serum albumin (BSA). Cells were incubated with RPMI/BSA containing 2 μM fura-2 acetoxymethy ester (fura-2/AM) for 1 h at room temperature and the excess of dye was washed with RPMI/BSA for 20 min. Glass coverslips bearing loaded cells were placed in a chamber on a Nikon Diaphot 300 microscope equipped for fluorescence. Thereafter, cells were treated with BSA or 0.1 μM VIP. Fura-2 fluorescence was excited at 340 or 380 nm and the emitted fluorescence was measured at 510 nm. $[Ca^{2+}]_i$ concentrations were calculated by an imaging system (Concord, Life Science Resources, TX, USA). The fluorescence ratio (340/380) was converted to $[Ca^{2+}]_i$ according to the formula derived from Grynkiewicz et al. [24], where R_{max} and R_{min} were determined using 2 μM Ionomicin and EGTA, respectively. All recordings were made at room temperature.

2.8. Detection of NE cell morphology

LNCaP cells (10^5 cells/well in six well plates) were stimulated with 0.1 μM VIP for 2 h after 1 h of pre-

treatment in the presence or absence of 60 μM BAPTA/AM. Thereafter, cells were photographed using Nikon Optiphot-2 (inverted and phase contrast microscopy). NE cells were considered as those bearing neurites of at least twice the cell body length.

2.9. Data analysis

The results are expressed either as the mean ± S.E. or as representative of three or more experiments. When appropriate, statistical analysis was performed using the Student's *t*-test. The level of significance was regarded as $P < 0.05$.

3. Results

3.1. VIP effect on c-fos oncogene mRNA expression

The mRNA expression of c-*fos* proto-oncogene in LNCaP cells was investigated by semi-quantitative RT-PCR with specific primers on total RNA extracted from cells (Fig. 1). As a control, the β-actin transcript was also analyzed. The amplification of RT reaction of RNA from unstimulated cells did not give any product, whereas the amplification from cells stimulated with 0.1 μM VIP gave a product of 612 bp that was sequenced and shown to correspond to c-*fos* oncogene. RT-PCR analysis (28 cycles) revealed an increased expression of c-*fos* mRNA in response to 0.1 μM VIP in a time dependent manner: mRNA levels increased at 30 min and decreased to basal values after 2 h.

3.2. Effect of VIP on c-fos oncogene protein

In order to evaluate if the changes in mRNA levels translated into changes in protein levels, the amount of c-*fos* protein in cells exposed to VIP was analyzed by Western blot. As shown in Fig. 2, VIP up-regulated c-Fos levels in nuclear fraction in a time-dependent manner. The maximal effect was seen at 1 h and then declined to control levels.

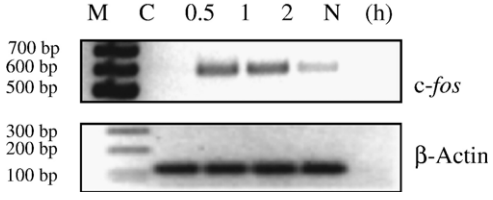

Fig. 1. Time-dependent expression of c-*fos* mRNA in LNCaP cells stimulated with 0.1 μM VIP. Total RNA was submitted to RT-PCR. Top: RT-PCR analysis of mRNA for c-*fos* gave a 612-bp band (top). Bottom: a 102-bp band corresponded to the housekeeping gene β-Actin as an internal control. C (control), N (no template), and M (bp marker) lanes are also shown. Results are representative of three separate experiments.

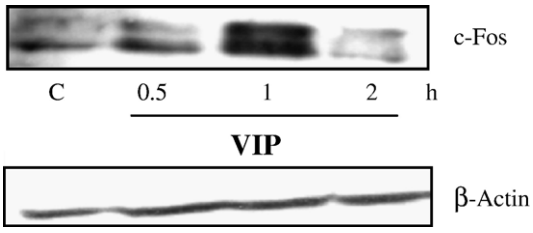

Fig. 2. Time-dependent expression of c-Fos protein in LNCaP cells stimulated with 0.1 μM VIP. The cells were harvested and nuclear extracts were prepared for Western blotting using specific antibodies to c-Fos and β-Actin. Results are representative of three separate experiments.

3.3. Role of VIP on intracellular Ca^{2+} levels

Next, we examined whether VIP modulated $[Ca^{2+}]_i$ levels in LNCaP cells. Fura-2 was used as the fluorescent calcium probe. As shown in Fig. 3, VIP increased intracellular Ca^{2+} levels in a time-dependent manner. After subtracting vehicle contribution, $[Ca^{2+}]_i$ levels elevated from a resting level of 35.5 ± 8.9 nM to 86.1 ± 6.8 nM after 45 min of 0.1 μM VIP stimulation ($n = 4$).

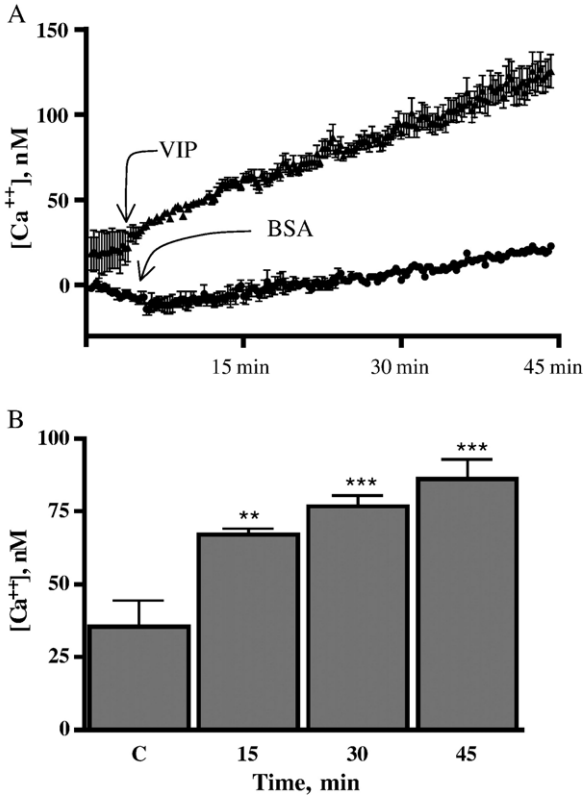

Fig. 3. Effect of VIP on $[Ca^{2+}]_i$ in LNCaP cells. (A) Time-course of fura-2 fluorescence was converted to calcium concentrations. VIP (0.1 μM) or BSA (5%) were perfused at point indicated by the arrows. The curve is representative of four separate experiments. (B) Comparison of results at 0, 15, 30, and 45 min. C (control) represents basal levels of $[Ca^{+2}]_i$ in LNCaP cells. RPMI-1640 supplemented with 5% BSA was used as a control for any response occurring as a result of vehicle addition. Data in each bar are the mean ± S.E. $^{**}P < 0.01$, $^{***}P < 0.001$ compared with control value in unstimulated cells ($n = 4$).

3.4. Involvement of intracellular Ca^{2+} in VIP-induced c-fos expression

We next explored the role of $[Ca^{2+}]_i$ in VIP stimulation of c-*fos* mRNA expression. LNCaP cells were treated with VIP after pre-incubation in the presence or in the absence of an intracellular Ca^{2+} chelator, BAPTA/AM. RT-PCR analysis (PCR was performed with 25 cycles) showed that pre-treatment of cells with 60 μM BAPTA/AM for 1 h decreased VIP-induced c-*fos* transcript to basal levels (Fig. 4), suggesting that $[Ca^{2+}]_i$ may play a significant role in mediating c-*fos* gene induction by VIP. Thereafter, Western blotting experiments were carried out in order to determine whether the BAPTA/AM effect on VIP-induced c-fos mRNA was accompanied by an inhibition on the VIP effect upon c-Fos protein levels. Fig. 5 shows that VIP up-regulated c-Fos levels in nuclear fraction, whereas BAPTA/AM reverted them to basal levels.

3.5. Involvement of intracellular Ca^{2+} in VIP-induced VEGF mRNA expression

Afterwards, we studied whether the VIP-induced increase of $[Ca^{2+}]_i$ levels was involved in the stimulatory effect of VIP on the expression of $VEGF_{165}$ mRNA. For this purpose, LNCaP cells were treated with VIP after pre-incubation in the presence or in the absence of the intracellular Ca^{2+} chelator BAPTA/AM. As shown in Fig. 6, quantitative real time RT-PCR experiments allowed us to detect a 43% inhibition of the VIP effect in the presence of BAPTA/AM.

3.6. Involvement of cAMP and Ca^{2+} in VIP effect on $VEGF_{165}$ production

We used H89 (a PKA inhibitor) and BAPTA/AM in order to determine whether PKA (of primary importance in cAMP signalling) and Ca^{2+} mediate the stimulatory effect of VIP on VEGF synthesis in LNCaP cells. As shown in Fig. 7, both molecules decreased VIP stimulation of

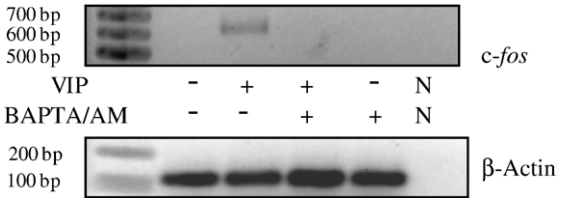

Fig. 4. (A) Role of $[Ca^{2+}]_i$ on the induction of c-*fos* expression by VIP. After pre-treatment for 1 h in the presence or absence of 60 μM BAPTA/AM, LNCaP cells were stimulated for 1 h with 0.1 μM VIP. Total RNA was submitted to RT-PCR. Semi-quantitative PCR was performed with 25 cycles to improve the detection of BAPTA/AM effect. (B) The expression of β-Actin was monitored as an internal control. A representative result from three independent experiments is shown.

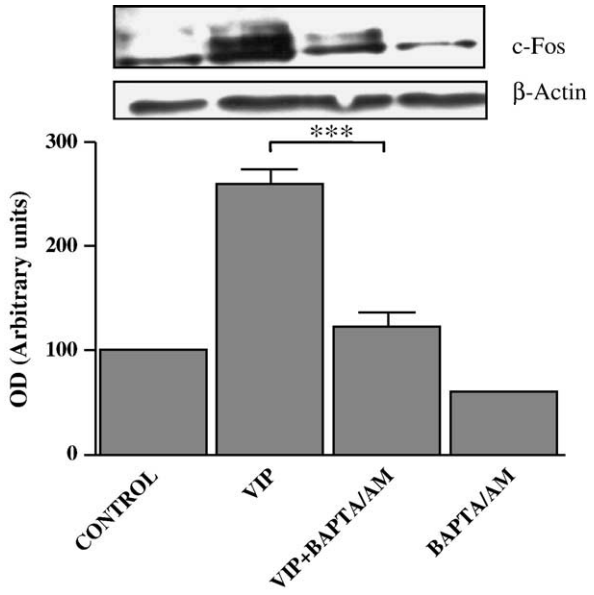

Fig. 5. Effect of BAPTA/AM on VIP-enhancing expression of c-Fos protein in LNCaP cells. Top: after pre-treatment for 1 h in the presence or absence of 60 μM BAPTA/AM, LNCaP cells were treated for 1 h with 0.1 μM VIP. Western blot analysis of c-Fos was performed in nuclear extracts. Data shown are representative of three independent experiments. (B) The intensities of c-Fos bands were normalized with those of β-Actin bands. Data in each bar are the mean ± S.E. $***P < 0.001$ ($n = 3$).

$VEGF_{165}$ levels, and the effect of VIP was completely abolished after cell pre-treatment with 10 μM H89 plus 60 μM BAPTA/AM. Indeed, BAPTA/AM inhibited $VEGF_{165}$ secretion in the absence of VIP stimulation, suggesting that constitutive activity of the Ca^{2+} pathway may contribute to basal VEGF production.

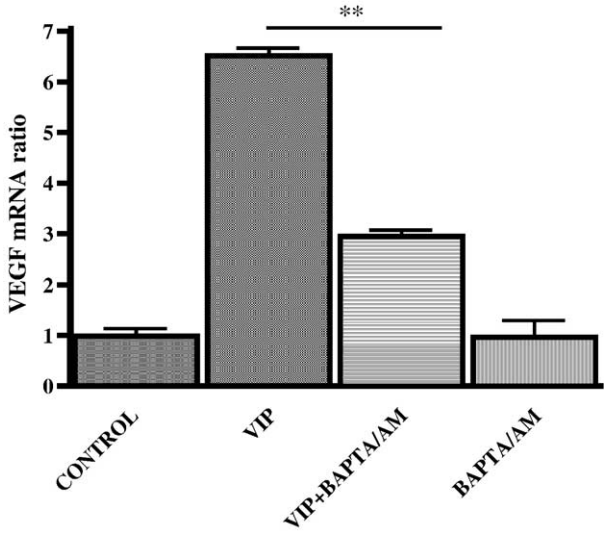

Fig. 6. Involvement of $[Ca^{+2}]_i$ in VIP effect on VEGF mRNA expression. After pre-treatment for 1 h in the presence or absence of 60 μM BAPTA/AM, LNCaP cells were stimulated for 1 h with 0.1 μM VIP. Total RNA was submitted to real-time RT-PCR quantification for $VEGF_{165}$ mRNA. Data in each bar are the mean ± S.E. $**P < 0.01$ ($n = 3$).

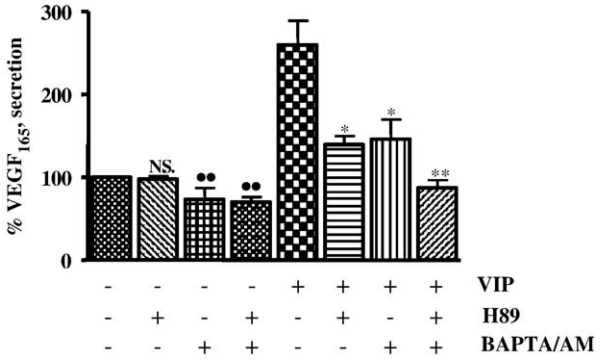

Fig. 7. Involvement of PKA and $[Ca^{+2}]_i$ in VIP effect on VEGF secretion. LNCaP cells were incubated with 10 μM H89 for 15 min and/or 60 μM BAPTA/AM for 1 h; thereafter, cells were stimulated with 0.1 μM VIP for 8 h. The supernatants were taken for VEGF assay by ELISA. Data in each bar are the mean ± S.E. ••$P<0.01$, *$P<0.05$, **$P<0.01$ (comparisons vs. the corresponding controls, $n=3$).

3.7. Involvement of AP-1 complex in VIP-induced VEGF mRNA expression

Thereafter, we used curcumin, which is an inhibitor of AP-1 binding [20], in order to study whether AP-1 activation is involved in VIP increase of VEGF mRNA levels. For this purpose, LNCaP cells were treated for 1 h with 0.1 μM VIP after 1 h of pre-incubation in the presence or in the absence of 10 μM curcumin. As shown in Fig. 8, curcumin led to a 40% inhibition of the VIP effect as detected by means of quantitative real time RT-PCR.

3.8. Involvement of AP-1 complex in VIP-induced VEGF secretion

To examine whether curcumin inhibition of VIP effect on expression of $VEGF_{165}$ mRNA was accompanied by an

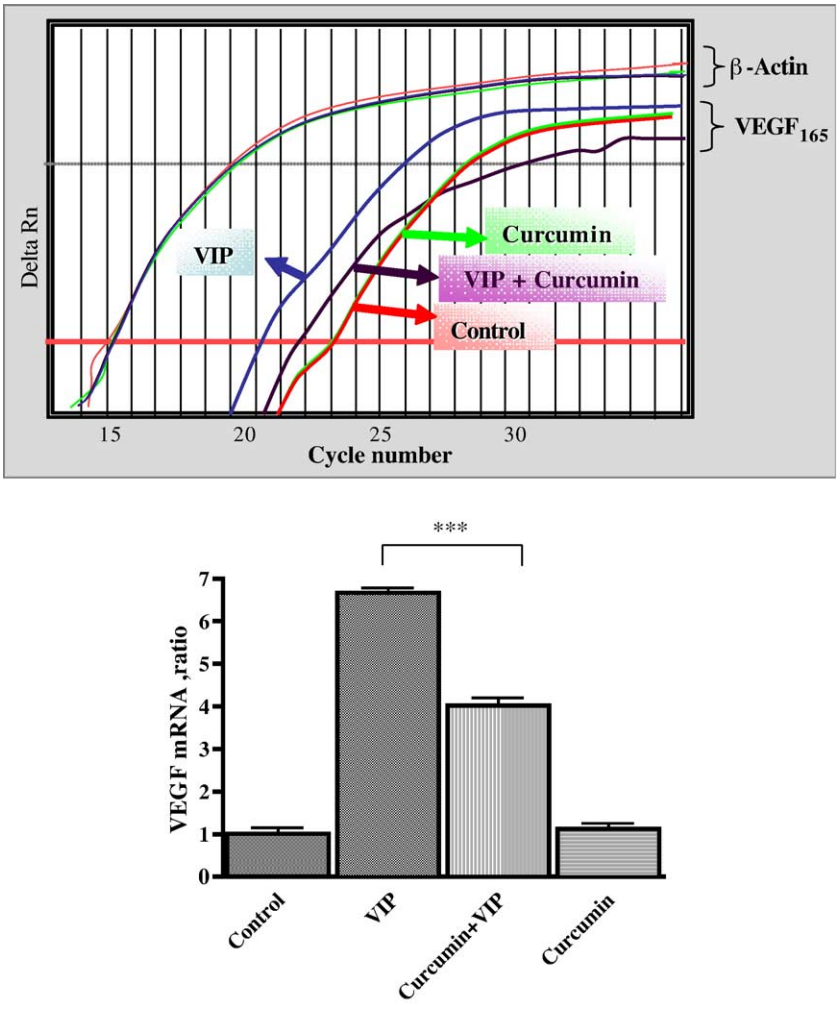

Fig. 8. Effect of curcumin on VIP-induced VEGF mRNA expression. After pre-treatment for 1 h in the presence or absence of 10 μM curcumin, LNCaP cells were stimulated for 1 h with 0.1 μM VIP. Total RNA was submitted to real-time RT-PCR quantification for $VEGF_{165}$ mRNA. Data in each bar are the mean ± S.E. ***$P<0.001$ ($n=3$).

inhibition on VEGF protein secretion, $VEGF_{165}$ levels in the culture medium were quantified by ELISA using LNCaP cells maintained in a conditioned medium. The pre-treatment with curcumin decreased VIP stimulation of $VEGF_{165}$ levels by 55% (Fig. 9).

3.9. Role of intracellular Ca^{2+} in VIP-induced NE cell differentiation

Finally, we assessed the possibility that the effect of VIP on $[Ca^{2+}]_i$ levels could be related to VIP-induction of NE cell differentiation. Following the same protocol, LNCaP cells were treated with VIP after pre-incubation in the presence or in the absence of BAPTA/AM. Thereafter, we measured the percentage of NE differentiated cells as those bearing neurites. Fig. 10 shows the morphological changes indicating that the inclusion of the intracellular Ca^{2+} chelator attenuated the VIP effect on NE differentiation although BAPTA/AM did not completely abolish it.

4. Discussion

We have previously demonstrated that VIP increases the expression of the major angiogenic factor (VEGF) as well as NE differentiation in human prostate cancer LNCaP cells [10] which suggests an involvement of VIP in prostate cancer progression from an androgen-dependent to an androgen-independent status. Whereas angiogenesis provides nutrients to tumour cells, NE cells produce growth factors in an autocrine/paracrine manner making possible that cancerous cells survive in androgen-independent conditions. In the present study, we analyzed the mechanisms that are responsible for the early effect of VIP on VEGF expression and NE differentiation in LNCaP cells.

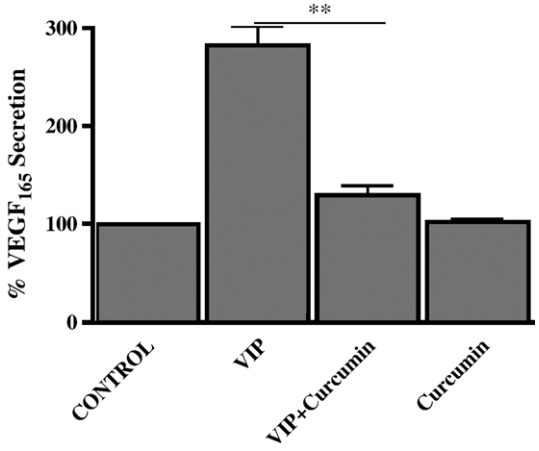

Fig. 9. Effect of curcumin on VIP-induced VEGF secretion. After pre-treatment for 1 h in the presence or absence of 10 μM curcumin, LNCaP cells were stimulated for 1 h with 0.1 μM VIP. Thereafter, the medium was assayed for $VEGF_{165}$ levels by ELISA. Data in each bar are the mean ± S.E. ***$P<0.001$ ($n=3$).

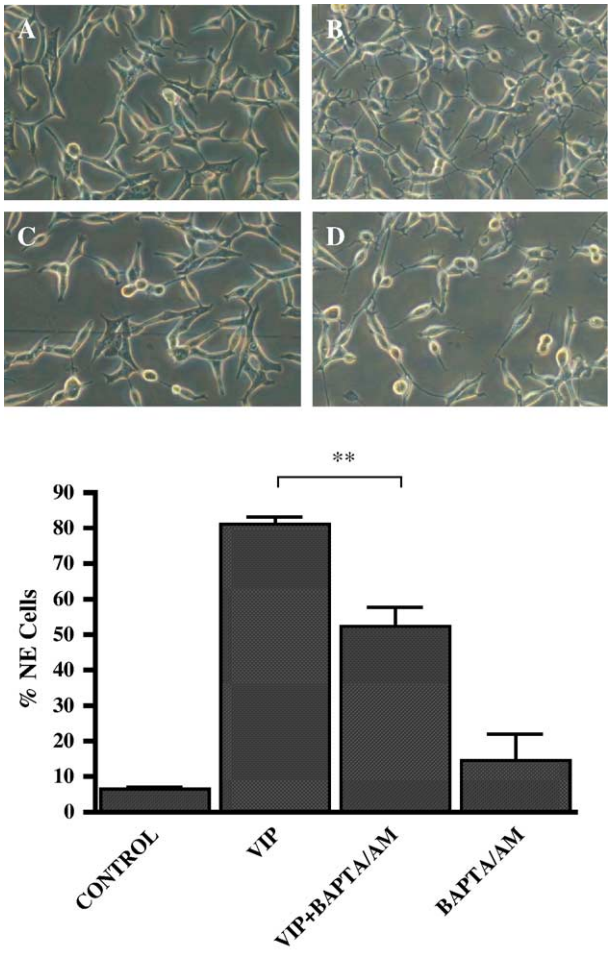

Fig. 10. Role of $[Ca^{+2}]_i$ on the induction of neurite outgrowth in LNCaP cells. Top: after pre-treatment for 1 h in the presence or absence of 60 μM BAPTA/AM, LNCaP cells were incubated for 2 h with 0.1 μM VIP. Panel A: control cells; B: cells were incubated 2 h with VIP; C: cells were incubated 1 h with BAPTA/AM, and then 2 h with 10% FBS; D: cells were incubated 1 h with BAPTA/AM, and then 2 h with VIP. Bottom: percentage of NE cells in LNCaP cultures. Each bar represents the mean ± S.E. values of three experiments performed in duplicate. **$P<0.01$ ($n=3$).

It is well established that $VAPC_1$ and $VPAC_2$ receptors are mainly coupled to Gs proteins resulting in activation of adenylyl cyclase but there is also evidence on VPAC receptor association to other signalling pathways downstream of cAMP or independent of cAMP [1]. In this context, VIP has been shown to increase prolactin secretion in cultured rat pituitary cells (GH_4C_1) via a cAMP-dependent mechanism which involves a transient elevation of intracellular Ca^{2+} [25]. Also, VIP was found to increase cytoplasmic calcium levels in blasts isolated from patients with myeloid leukaemia [26]. Moreover, VIP induced c-*fos* mRNA expression in GH_3 pituitary tumour cells but this effect was not mimicked by the cAMP analogue 8-Br-cAMP, suggesting that signals other than, or in addition to cAMP mediate VIP-stimulated c-*fos* gene expression [27]. In addition to these observations, VIP has been reported to increase intracellular Ca^{2+} levels in hamster CHO ovary cells, the effect being higher in $VPAC_1$ than in $VPAC_2$

receptor expressing cells [6]. The efficient coupling of the $VPAC_1$ receptor to $[Ca^{2+}]_i$ increase has been attributed to a small sequence in its third intracellular loop that probably interacts with $G\alpha_i$ and $G\alpha_q$ proteins [5]. In this context, the involvement of the recently characterized family of receptor activity modifying proteins (RAMP) [28] must be considered since RAMP expression has been demonstrated in human prostate hyperplasias and carcinomas as well as in the prostate carcinoma-derived cell lines PC3 and DU145 [29]. Interestingly, RAMP2 forms a heterodimer with $VPAC_1$ receptor in COS-7 cells resulting in a specific augmentation of $VPAC_1$ receptor-mediated signalling through the phosphoinositol (PI) hydrolysis pathway with no alteration in $VPAC_1$ receptor-mediated induction of cAMP signalling [30]. Since data on RAMP expression and function in LNCaP cells are still unavailable, the present demonstration of coupling of VIP receptors to the Ca^{2+} signalling pathway makes advisable to address that point in further studies. Our previous results in LNCaP cells also support that $VPAC_1$ is the main VIP receptor since it appears to initiate the mechanisms of VIP-induction of both VEGF expression and NE cell differentiation [10]. In the present work, we observed that the stimulation of VEGF expression by VIP is mediated, as least in part, by AP-1 transcription factor since curcumin (an inhibitor of AP-1 binding), was able to inhibit VIP-induction of VEGF expression at both mRNA and protein levels. VIP enhanced the expression of both c-*fos* mRNA and protein (at 30 min and 1 h, respectively) in LNCaP cells. Moreover, VIP-stimulated c-*fos* expression was abolished by 89% in the presence of an intracellular Ca^{2+} chelator, BAPTA/AM. These results support the involvement of Ca^{2+} in VIP signalling in LNCaP cells.

There is substantial evidence suggesting an important role for calcium during tumorigenesis. Many mitogens and tumour growth factors elicit rapid elevations of intracellular calcium [31–33]. Furthermore, calcium is involved in events that regulate cell cycle progression, angiogenesis, and apoptosis in various cell systems [34–36]. The importance of calcium homeostasis to malignant cells has been underscored by studies showing that antagonists of the phosphatidylinositol pathway [37] or calcium influx [36] can arrest the growth of a variety of tumour cells cultured in vitro or as in vivo tumour xenografts. Until recently, the problems of normal and pathological development of the human prostate have mainly been addressed from biochemical and molecular biology perspectives, whereas the roles of Ca^{2+} signalling and even more plasma membrane ion channels have been largely ignored [38,39].

Prostate cancer, one of the leading threats to man's health, progresses from an early stage, which depends on androgens for growth and survival so that androgen ablation therapy may cause tumour to regress at this time, to the late androgen-independent stage, for which there is currently no successful therapy [15,40]. It is therefore extremely important to understand what drives the progression to androgen independence. This undesired transformation is associated with the appearance of new cell phenotypes which result in angiogenesis, NE differentiation, and inhibition of apoptosis [15,40]. After our previous observations on VIP involvement in prostate cancer, i.e., VIP induction of VEGF expression and NE differentiation in LNCaP cells [10], we have analyzed in the present work if these effects are associated with VIP enhancement of intracellular calcium levels. In this regard, the 0.1 μM dose of VIP used to induce increasing of intracellular Ca^{2+} concentration is similar to that previously shown to result in maximal cAMP production and full occupation of receptors in the same cell system [11]. We detected that cell pre-treatment with the calcium chelator BAPTA/AM was able to inhibit in a similar extent the effect of this neuropeptide on the expression of both $VEGF_{165}$ mRNA (by 43%) and protein (by 46%) and NE cell differentiation (by 37%). Moreover, this partial inhibition of the two events allows thinking in a signalling pathway of VIP that could be mediated through cooperation between the traditional second messenger cAMP and $[Ca^{2+}]_i$ increase in prostate LNCaP cancer cells. This possibility is reinforced by present results on complete blocking of VIP effect on $VEGF_{165}$ protein production by simultaneous cell treatment with the PKA inhibitor H89 and the calcium chelator BAPTA/AM (each agent alone led only to partial inhibition of VIP response). In other context, the lack of effect of BAPTA/AM alone on $VEGF_{165}$ mRNA expression discards the possibility of a generalised toxic effect of the intracellular Ca^{2+} chelator on transcriptional activity. Indeed, toxic actions of BAPTA/AM are unlikely since it did not modify both cell morphology and cell death extent. Finally, the implication of c-Fos on the induction of the main angiogenic factor VEGF is possible because the promoter region of VEGF gene has five AP-1 response elements [21]. This fact represents a link between a nuclear oncogene, angiogenesis, and NE differentiation through a dependence on the initiating signal of VIP acting through $VPAC_1$ receptors. The present observations are a contribution to the understanding of the various effects of the VIP-mediated response in prostate LNCaP cancer cells.

Acknowledgements

This study has been supported by grants from the Ministerio de Educación y Ciencia (SAF2001-1025 and SAF2004-4933) and the Comunidad Autónoma de Madrid (GR/SAL/0781/2004). B.C. and M.G.S. are fellows from the Ministerio de Educación y Ciencia.

References

[1] M. Laburthe, A. Couvineau, Molecular pharmacology and structure of VPAC receptors for VIP and PACAP, Regul. Pept. 108 (2002) 165–173.

[2] M.J. Carmena, J.C. Prieto, Cyclic AMP-stimulating effect of vasoactive intestinal peptide in isolated epithelial cells of rat ventral prostate, Biochim. Biophys. Acta 463 (1983) 414–418.
[3] R.M. Solano, M.J. Carmena, I. Carrero, S. Cavallaro, F. Roman, C. Hueso, S. Travali, N. Lopez-Fraile, L.G. Guijarro, J.C. Prieto, Characterization of vasoactive intestinal peptide/pituitary adenylate cyclase-activating peptide receptors in human benign hyperplastic prostate, Endocrinology 137 (1996) 2815–2822.
[4] N.N. Huang, D.J. Wang, L.A. Heppel, Role of adenosine 3′:5′-monophosphate-dependent protein kinase and cAMP levels in ATP-dependent mitogenesis in Swiss 3T3 cells, J. Biol. Chem. 269 (1994) 548–555.
[5] I. Langer, P. Vertongen, J. Perret, M. Waelbroeck, P. Robberecht, A small sequence in the third intracellular loop of the VPAC(1) receptor is responsible for its efficient coupling to the calcium effector, Mol. Endocrinol. 16 (2002) 1089–1096.
[6] I. Langer, J. Perret, P. Vertongen, M. Waelbroeck, P. Robberecht, Vasoactive intestinal peptide (VIP) stimulates $[Ca^{2+}]_i$ and cyclic AMP in CHO cells expressing $G\alpha_{16}$, Cell Calcium 30 (2001) 229–234.
[7] W.I. DeHaven, J. Cuevas, VPAC receptor modulation of neuro-excitability in intracardiac neurons: dependence on intracellular calcium mobilization and synergistic enhancement by PAC1 receptor activation, J. Biol. Chem. 279 (2004) 40609–40621.
[8] H. Kamaishi, T. Heñido, T. Suzuki, Multiple signal pathways coupling VIP and PACAP receptors to calcium channels in hamster submandibular ganglion neurons, Auton. Neurosci. 111 (2004) 15–26.
[9] T.W. Moody, J.M. Hill, R.T. Jensen, VIP as a trophic factor in the CNS and cancer cells, Peptides 24 (2003) 163–177.
[10] B. Collado, I. Gutierrez-Cañas, N. Rodriguez-Henche, J.C. Prieto, M.J. Carmena, Vasoactive intestinal peptide increases vascular endothelial growth factor expression and neuroendocrine differentiation in human prostate cancer LNCaP cells, Regul. Pept. 119 (2004) 69–75.
[11] M.G. Juarranz, O. Bolaños, I. Gutiérrez-Cañas, E.A. Lerner, P. Robberecht, M.J. Carmena, J.C. Prieto, N. Rodríguez-Henche, Neuroendocrine differentiation of the LNCaP prostate cancer cell line maintains the expression and function of VIP and PACAP receptors, Cell. Signal. 13 (2001) 887–894.
[12] I. Gutiérrez-Cañas, N. Rodríguez-Henche, O. Bolaños, M.J. Carmena, J.C. Prieto, M.G. Juarranz, VIP and PACAP are autocrine factors that protect the androgen-independent prostate cancer cell line PC-3 from apoptosis induced by serum withdrawal, Br. J. Pharmacol. 139 (2003) 1050–1058.
[13] T. Iwata, O. Ukimura, M. Inaba, M. Kojima, K. Kumamoto, H. Ozawa, M. Kawata, T. Miki, Immunohistochemical studies on the distribution of nerve fibers in the human prostate with special reference to the anterior fibromuscular stroma, Prostate 48 (2001) 242–247.
[14] A. Plonowski, J.L. Varga, A.V. Schally, M. Krupa, K. Groot, G. Halmos, Inhibition of PC-3 human prostate cancers by analogs of growth hormone-releasing hormone (GH-RH) endowed with vasoactive intestinal peptide (VIP) antagonistic activity, Int. J. Cancer 98 (2002) 624–629.
[15] E. Deutsch, L. Maggiorella, P. Eschwege, J. Bourhis, J.C. Soria, B. Abdulkarim, Environmental, genetic, and molecular features of prostate cancer, Lancet Oncol. 5 (2004) 303–313.
[16] M.G. Juarranz, P. De Neef, P. Robberecht, Vasoactive intestinal polypeptide receptor VPAC(1) subtype is predominant in rat prostate membranes, Prostate 41 (1999) 1–6.
[17] Y.C. Jang, L.S. Kao, F.F. Wang, Involvement of Ca2+ signalling in the vasoactive intestinal peptide and 8-Br-cAMP induction of c-fos mRNA expression, Cell. Signal. 10 (1998) 27–34.
[18] H. Schafer, J. Zheng, F. Gundlach, R. Gunther, W.E. Schmidt, PACAP stimulates transcription of c-Fos and c-Jun and activates the AP-1 transcription factor in rat pancreatic carcinoma cells, Biochem. Biophys. Res. Commun. 221 (1996) 111–116.
[19] R. Eferl, E.F. Wagner, AP-1: a double-edged sword in tumorigenesis, Nat. Rev., Cancer 3 (2003) 859–868.
[20] E.R. Hahm, Y.S. Gho, S. Park, C. Park, K.W. Kim, C.H. Yang, Synthetic curcumin analogs inhibit activator protein-1 transcription and tumor-induced angiogenesis, Biochim. Biophys. Res. Commun. 321 (2004) 337–344.
[21] N.S. Levy, M.A. Goldberg, A.P. Levy, Sequencing of the human vascular endothelial growth factor (VEGF) 3′ untranslated region (UTR): conservation of five hypoxia-inducible RNA–protein binding sites, Biochim. Biophys. Acta 1352 (1997) 167–173.
[22] J.T. Chang, I.H. Chen, C.T. Liao, H.M. Wang, Y.M. Hsu, K.F. Hung, C.J. Lin, L.L. Hsieh, A.J. Cheng, A reverse transcription comparative real-time PCR method for quantitative detection of angiogenic growth factors in head and neck cancer patients, Clin. Biochem. 35 (2002) 591–596.
[23] N.J. Mabjeesh, M.T. Willard, C.E. Frederickson, H. Zhong, J.W. Simons, Androgens stimulate hypoxia-inducible factor 1 activation via autocrine loop of tyrosine kinase receptor/phosphatidylinositol 3′-kinase/protein kinase B in prostate cancer cells, Clin. Cancer Res. 9 (2003) 2416–2425.
[24] G. Grynkiewicz, M. Poenie, R.Y. Tsien, A new generation of Ca2+ indicators with greatly improved fluorescence properties, J. Biol. Chem. 260 (1985) 3440–3450.
[25] T. Bjoro, B.C. Ostberg, O. Sand, J. Gordeladze, J.G. Iversen, P.A. Torjesen, K.M. Gautvik, E. Haug, Vasoactive intestinal peptide and peptide with N-terminal histidine and C-terminal isoleucine increase prolactin secretion in cultured rat pituitary cells (GH4C1) via a cAMP-dependent mechanism which involves transient elevation of intracellular Ca2+, Mol. Cell. Endocrinol. 49 (1987) 119–128.
[26] N. Hayez, I. Harfi, R. Lema-Kisoka, M. Svoboda, F. Corazza, E. Sariban, The neuropeptides vasoactive intestinal peptide (VIP) and pituitary adenylate cyclase activating polypeptide (PACAP) modulate several biochemical pathways in human leukemic myeloid cells, J. Neuroimmunol. 149 (2004) 167–181.
[27] J.H. Lin, Y.C. Jang, D.C. Wen, F.F. Wang, Synergistic activation of cAMP and calcium on cAMP-response-element-mediated gene expression in GH3 pituitary tumor cells, Cell. Signal. 8 (1996) 111–115.
[28] M. Udawela, D.L. Hay, P.M. Sexton, The receptor activity modifying protein family of G protein coupled receptor accessory proteins, Semin. Cell Dev. Biol. 15 (2004) 299–308.
[29] G. Mazzocchi, L.K. Malendowicz, A. Ziolkowska, R. Spinazzi, P. Rebuffat, F. Aragona, E. Ferrazzi, P.P. Parnigotto, G.G. Nussdorfer, Adrenomedullin (AM) and AM receptor type 2 expression is up-regulated in prostate carcinomas (PC), and AM stimulates in vitro growth of a PC-derived cell line by enhancing proliferation and decreasing apoptosis rates, Int. J. Oncol. 25 (2004) 1781–1787.
[30] A. Christopoulos, G. Christopoulos, M. Morfis, M. Udawela, M. Laburthe, A. Couvineau, K. Kuwasako, N. Tilakaratne, P.M. Sexton, Novel receptor partners and function of receptor activity-modifying proteins, J. Biol. Chem. 278 (2003) 3293–3297.
[31] M.J. Berridge, Inositol trisphosphate and calcium signalling, Nature 361 (1993) 315–325.
[32] K. Cole, E. Kohn, Calcium-mediated signal transduction: biology, biochemistry, and therapy, Cancer Metastasis Rev. 13 (1994) 31–44.
[33] A.R. Means, Calcium, calmodulin and cell cycle regulation, FEBS Lett. 347 (1994) 1–4.
[34] E.C. Kohn, R. Alessandro, J. Spoonster, R.P. Wersto, L.A. Liotta, Angiogenesis: role of calcium-mediated signal transduction, Proc. Natl. Acad. Sci. U. S. A. 92 (1995) 1307–1311.
[35] P. Nicotera, B. Zhivotovsky, S. Orrenius, Nuclear calcium transport and the role of calcium in apoptosis, Cell Calcium 16 (1994) 279–288.
[36] M.J. Berridge, M.D. Bootman, P. Lipp, Calcium—A life and death signal, Nature 395 (1998) 645–648.
[37] G. Powis, D. Phil, Inhibitors of phosphatidylinositol signalling as antiproliferative agents, Cancer Metastasis Rev. 13 (1994) 91–103.

[38] F. Vanden Abeele, Y. Shuba, M. Roudbaraki, L. Lemonnier, K. Vanoverberghe, P. Mariot, R. Skryma, N. Prevarskaya, Store-operated Ca2+ channels in prostate cancer epithelial cells: function, regulation, and role in carcinogenesis, Cell Calcium 33 (2003) 357–373.
[39] K. Vanoverberghe, F. Vanden Abeele, P. Mariot, G. Lepage, M. Roudbaraki, J.L. Bonnal, B. Mauroy, Y. Shuba, R. Skryma, N. Prevarskaya, Ca2+ homeostasis and apoptotic resistance of neuroendocrine-differentiated prostate cancer cells, Cell Death Differ. 11 (2004) 321–330.
[40] C.N. Sternberg, Highlights of contemporary issues in the medical management of prostate cancer, Crit. Rev. Oncol./Hematol. 43 (2002) 105–121.